

DIELECTRIC WAVEGUIDE OPTIMIZATION FOR THE ENHANCEMENT OF TE-POLARIZATION TRANSMISSION OF PLASMONICS-BASED MSM-PD

Ayman Karar¹, Chee Leong Tan², Kamal Alameh^{1,4}, Yong Tak Lee^{2,3,4}

¹Electron Science Research Institute, Edith Cowan University, AU.

²School of Photonics Science, Gwangju Institute of Science and Technology (GIST),
Gwangju, Republic of Korea

³Department of Information and Communications, GIST, Republic of Korea.

⁴Department of Nanobio Materials and Electronics, World Class University (WCU),
GIST, Republic of Korea

a.karar@ecu.edu.au, ccheelong@gist.ac.kr, k.alameh@ecu.edu.au, ytle@gist.ac.kr

PACS 42.25.Bs, 42.25.Ja, 73.50.Pz

In this paper, we use the finite difference time-domain (FDTD) method to optimize the TE-polarized light transmission of a metal-semiconductor-metal photodetector (MSM-PD) employing a dielectric waveguide on top of metal nano-gratings. Simulation results demonstrate that the funneling transmission of the TE-polarized light through the nanoslit of the MSM-PD structure is highly dependent on the structure geometries, such as the waveguide and nano-grating heights. We also demonstrate that adding a dielectric waveguide layer on top of the nano-metal gratings supports both the TM- and TE polarizations, and enhances the light transmission for TE-polarization around 3-times in comparison with conventional plasmonics MSM-PD structures.

Keywords: FDTD simulation, MSM-PD, waveguide, plasmonics, nano-gratings, surface plasmon.

1. Introduction

Metal-semiconductor-metal photodetectors (MSM-PDs) have several attractive features, such as high speed, ease of fabrication and monolithic integration with VLSI circuitry, which make them an excellent candidate for application in high-speed optical interconnects, high-speed sampling, and ultra-high speed optical fibre communications [1, 2]. For very high-speed applications, the MSM-PD is a better option than a p-i-n PD, since the real capacitance of the MSM-PD's interdigitated electrode geometry is much lower than that of a p-i-n PD of comparable size [3].

Typically, the speed of the MSM-PD is largely limited by the transit time of the photo-generated carriers. Scaling down the distance between the interdigital contacts and overall dimensions of the MSM-PD has been the most common way to increase the photodetector speed [4, 5]. By decreasing the spacing between the electrode fingers down to the optical diffraction limit, the response time could be reduced to tens of picoseconds [6]. However, the surface reflectivity and the shadowing effect of the metal fingers prevent conventional MSM-PDs from achieving external quantum efficiency greater than 50% for equal electrode width and spacing. This is due to the blocking of light by the detector's interdigitated finger structure.

Since Ebbesen et al. [7] reported extraordinary optical transmission (EOT) of periodic metal aperture arrays through surface plasmons, many efforts have been devoted

to exploring the EOT through metallic gratings [8, 9]. Later, it was demonstrated experimentally that the transmission of light through a sub-wavelength slit structure can be enhanced if the metal is patterned as nano-gratings, which enable the incident light to couple into surface plasmon polaritons (SPPs) propagating at the interface between metal and the air, thus focusing the light into the sub-wavelength slit [10, 11].

Recently, several MSM-PD structures, driven by TM-polarized light and based on nano-patterned metal fingers, have been reported to demonstrate substantial transmission enhancement through the excitation and guidance of SPPs into the photodetector slits [12, 13]. For example, the MSM-PD comprising Ag/GaAs nano-gratings reported by Collin et al. [14] exhibited a cut off frequency greater than 300 GHz and a quantum efficiency exceeding 50%. Lee et al. have reported a plasmonic metal photonic crystal (MPC) integrated on a quantum dot infrared photodetector demonstrating more than 2-times enhancement in detectivity [15].

Since there is no cut-off wavelength for the fundamental TM-polarized slit mode, it is possible to achieve extraordinary transmission with almost any sub-wavelength slit width. However, since the SPPs are TM-polarized mode, only the TM-polarization component of the incident light can be resonantly enhanced via transmission through the subwavelength slits. In this case, sub-wavelength slits act as polarization selector, which means that the penetration of the TE-polarized mode is suppressed. Furthermore, the TE-polarized mode intrinsically has a cut-off wavelength, making such MSM-PD structures polarization sensitive, and hence, less attractive for applications requiring polarization insensitive operation.

In this paper, we use the FDTD analysis to optimize a novel MSM-PD structure employing a dielectric thin layer waveguide deposited onto nano-patterned metal fingers. Our simulation results demonstrate 3-times enhancement in TE-polarized light transmission in comparison with conventional MSM-PDs.

2. Design of MSM-PD with enhanced TE-polarization transmission

Recently, a MSM-PD structure based on the deposition of a dielectric layer on top of metal fingers has been proposed by Nikitin et al. using the coupled mode method [16]. This was subsequently developed by Guillaumée et al., who experimentally demonstrated transmission enhancement for TE-polarized light through a subwavelength slit [17]. However, such a structure is sensitive to two parameters, namely, the height of the dielectric layer as well as the periodicity of the nano-patterned metal gratings, which were not fully optimised. In this paper, we investigate and optimize the key parameters of the dielectric-based MSM-PD structure, shown in Figure 1(a), to maximise the transmission of both the TE- and TM- polarized modes. The dielectric waveguide based MSM-PD structure consists of a subwavelength aperture of width X_w sandwiched between linear metal nano-gratings of heights h_g , and a period (Λ). The entire structure is grown on top of a semiconductor substrate. The metal contact is covered with a thin dielectric film with height h_{WG} . The presence of a thin dielectric layer on top of patterned metal gratings allows a TE-polarized incident light to couple to the dielectric waveguide modes and be guided towards the slit. At the same time, the extraordinary transmission of the TM-polarised light is maintained.

A 2D Finite Difference Time Domain (FDTD) software developed by Optiwave Inc was used to simulate the structure shown in Figure 1(a). A mesh step size of 10 nm was used in the simulation, with a time step satisfying the condition $\delta t < 0.1\delta_x/c$, where δ_x is the mesh size and c is the speed of light. This high-resolution sampling yielded solutions that converged at reasonable computation times. The excitation field was modeled as a

Gaussian-modulated continuous plane wave in the x-direction. The anisotropic perfectly matched layer (APML) boundary conditions were applied in both the x- and z- directions to accurately simulate the light reflected off both sides, as well as the light reflected off the top and bottom surface of the MSM-PD structure. In all the simulations, the light wave was normally incident on the top surface of the metal nano-gratings site. The gold (Au) dielectric permittivity was defined by the Lorentz-Drude model [3] and the refractive index for the dielectric layer was chosen to be 2.3, mainly to demonstrate the concept of TE-polarized light transmission enhancement.

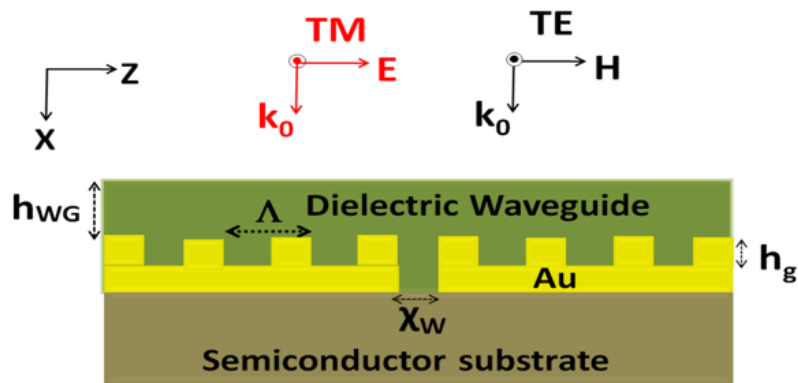
The TE and TM transmission spectra for two MSM-PD structures (without a dielectric waveguide), one with and the other without metal nano-gratings, are shown in Figure 1(b). An essential difference between the spectra for the TM- and TE- polarizations is already noticeable for a single slit without metal nano-gratings. While the TM-polarized mode spectra show interlaced maxima associated with the Fabry-Perot slit waveguide resonance, the TE-polarized mode resonance maxima display a rapid fall-off, due to the slit mode cut-off seen at longer wavelengths. No significant difference was noted in the TE-polarized mode transmission spectra for the structure with and without metal nano-gratings. However, the TM mode was resonantly enhanced by using the nano-gratings. Figure 1(c) shows the measured I-V characteristics for a nano-grating-patterned GaAs MSM-PD illuminated with 6.42 mW of laser power, for two input polarization states that correspond to the maximum, i.e. TM mode (dashed-dot), and minimum, i.e. TE mode (dashed), possible measured photocurrents, respectively. These results indirectly reveal the polarization dependent loss of the plasmonics-based MSM-PD device.

3. Results and discussion

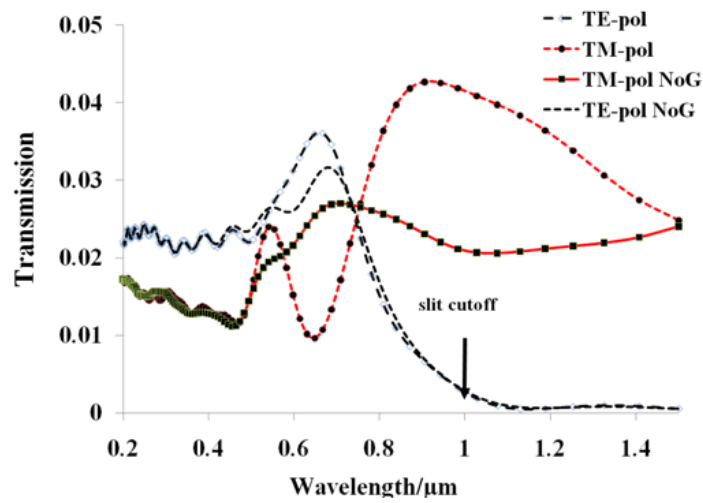
Several parameters of the dielectric-waveguide-based MSM-PD structure were optimized. These parameters are the nano-grating height, h_g , nano-grating period, Λ , waveguide height, h_{WG} , duty cycle of the nano-gratings. Each parameter was varied over a certain range of values, while all other parameters were kept constant. Initially, we used the structure shown in Figure 1(a) with metal nano-gratings to optimize the waveguide height h_{WG} . The dielectric waveguide height was varied, while keeping the subwavelength aperture width X_w and h_g constant at 430 nm and 200 nm, respectively. Moreover, the duty cycle, grating period and pitch number were kept at 0.5, 830 nm and 7, respectively.

Figure 2(a) illustrates the TE-polarized transmission spectra with no dielectric waveguide, 150 nm, 200 nm and 250 nm waveguide height. It is apparent from Figure 2(a) that the dielectric waveguide not only affects the amount of the light flux transmitted through the slit, but also the peak resonance wavelength. This indicates that the dielectric layer allows the incident light to resonantly couple to the metal nano-gratings. As seen from Figure 2(a), the resonance peak was highly dependent on the waveguide height and was red-shifted with increasing the waveguide height. Keeping the dielectric waveguide height at 200 nm and the other parameters constant, the simulated TE-polarized transmission spectra, shown in Figure 2(b), was evaluated for metal nano-grating height from 50 nm to 200 nm. As seen in Figure 2(b) while the metal nano-grating height affected the TE-polarized light transmission flux, it had no impact on the resonance wavelength. It was also noted that the transmission peak increases with decreasing the metal nano-grating height.

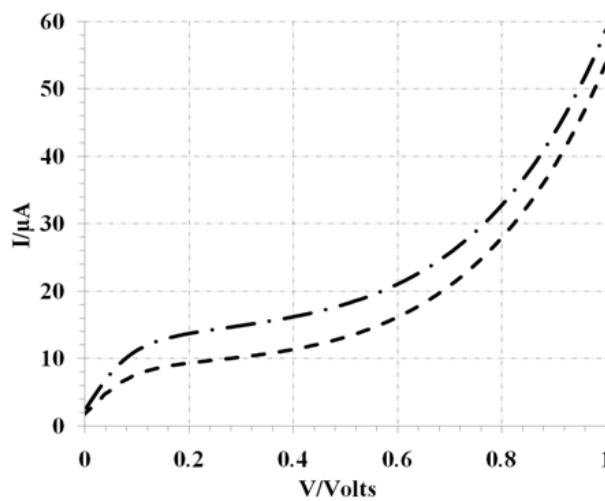
Figures 3(a and b) show the simulated TE-polarization transmission spectra for different metal nano-grating periods, and duty cycles, for a slit width of 430 nm, a nano-grating height of 50 nm and a dielectric waveguide height of 200 nm. The duty cycle



(a)

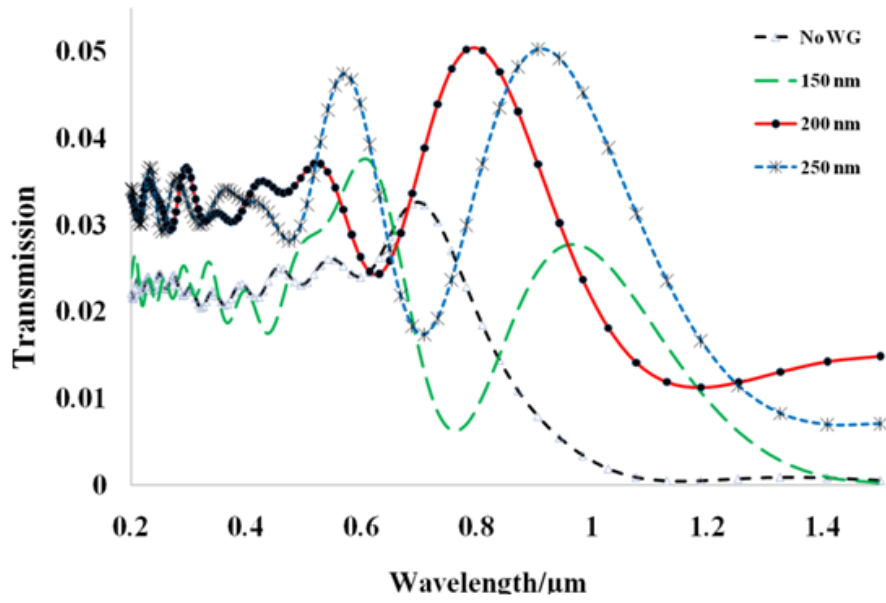


(b)

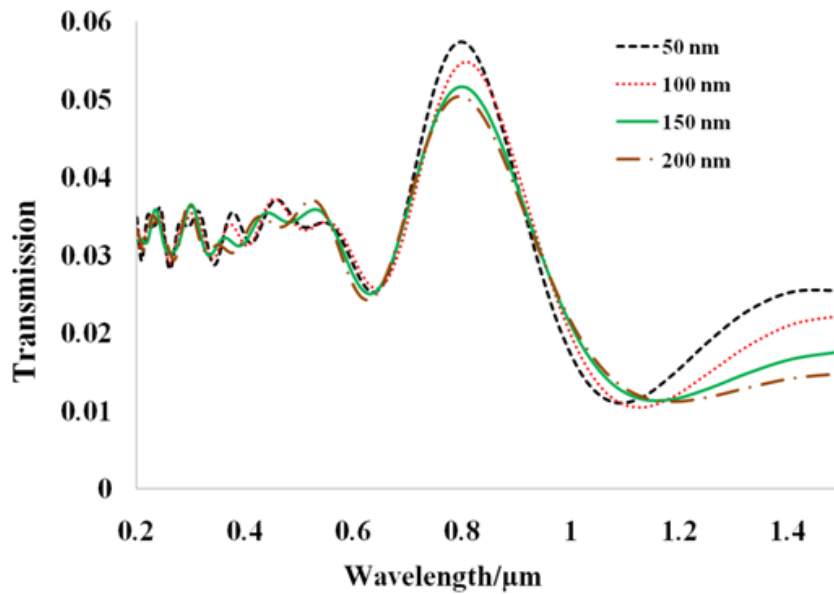


(c)

Fig. 1. **a)** 2-dimensional schematic of the dielectric-based MSM-PD structure, **b)** transmission spectra of two structures without dielectric waveguides, for fingers with and without metal nano-gratings, **c)** I-V characteristics of the MSM-PD with nano-gratings for TE- and TM-polarized input laser beams of power 6.42 mW

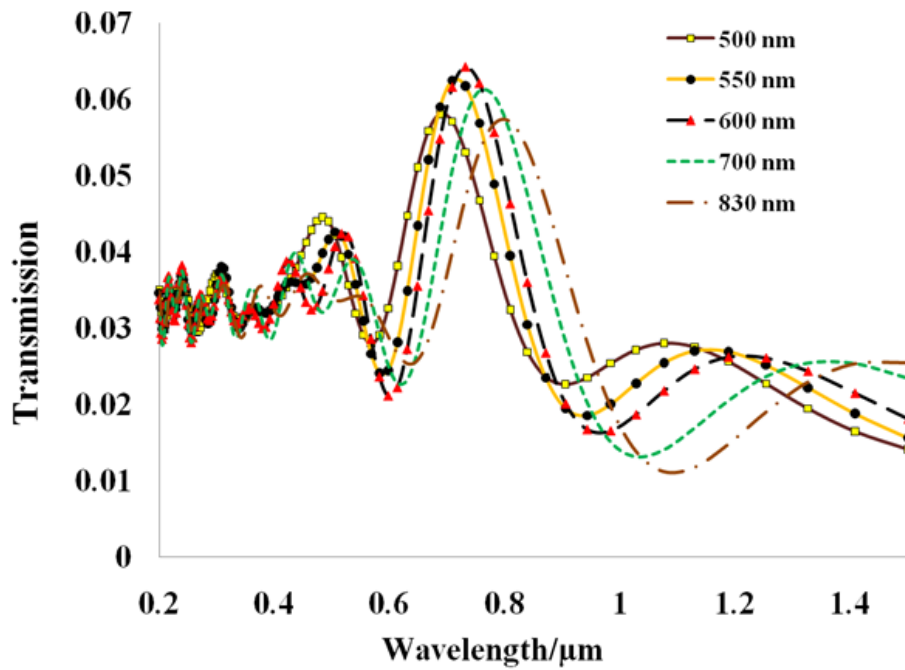


(a)

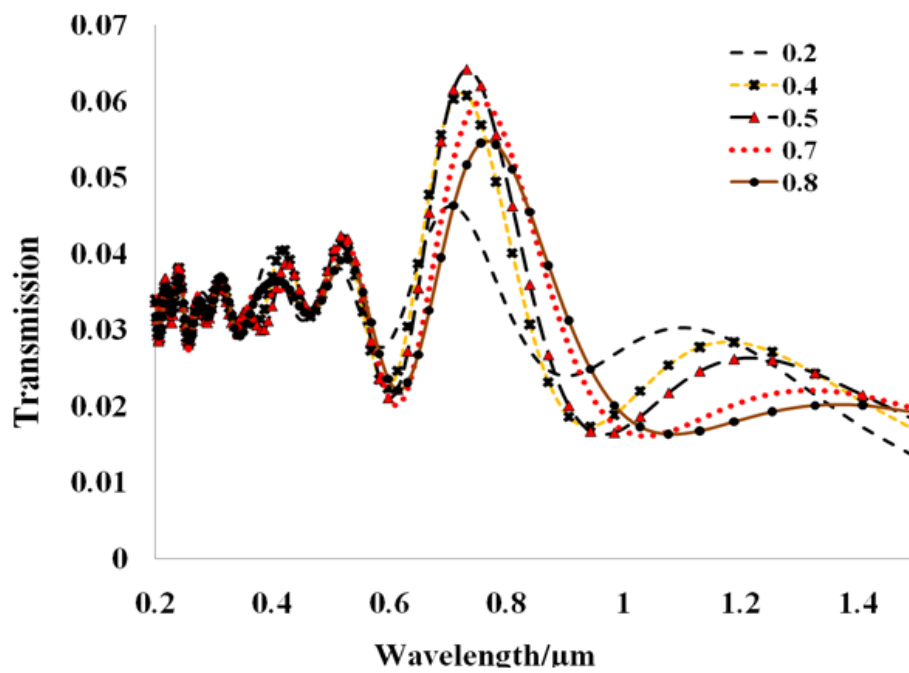


(b)

Fig. 2. Simulated TE-polarization transmission spectra for different **a)** dielectric waveguide height and, **b)** nano-grating height. The slit width was 430 nm



(a)



(b)

Fig. 3. Simulated TE-polarisation transmission spectra for different **a)** periodicity and, **b)** duty cycle with 430 nm slit width, 50 nm nano-grating height and 200 nm dielectric waveguide height

is defined as the ratio of the nano-grating line width to the period, Λ . It is seen from Figure 3(a) that the resonance peak of the TE-polarized light transmission was red-shifted when the periodicity increased. The maximum attainable transmission peak occurred at 730 nm for a nano-grating period of 600 nm. Figure 3(b) shows that the nano-grating duty cycle had a significant impact on both the transmission peak and the resonance wavelength, and that the resonance wavelength was red-shifted when the duty cycle increased, while the maximum transmission occurred when the duty cycle was 50%.

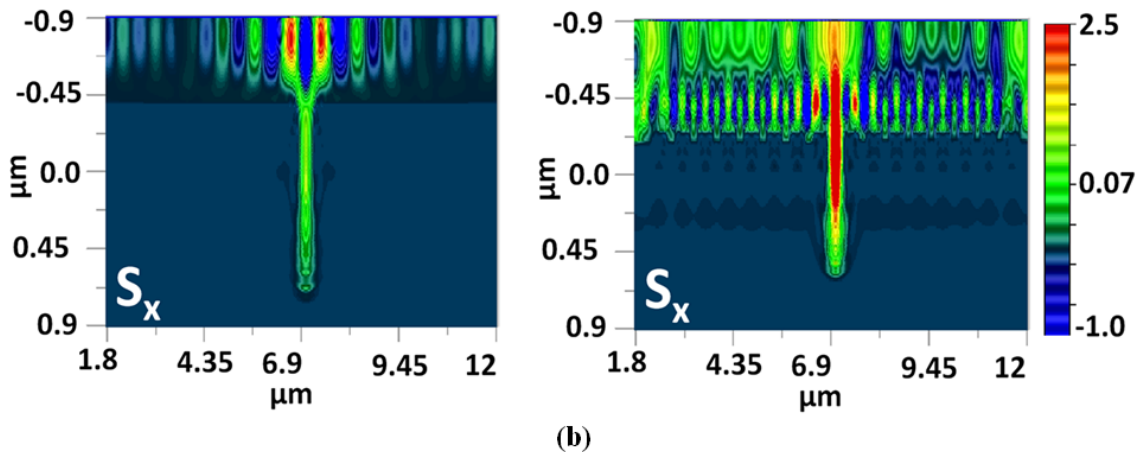
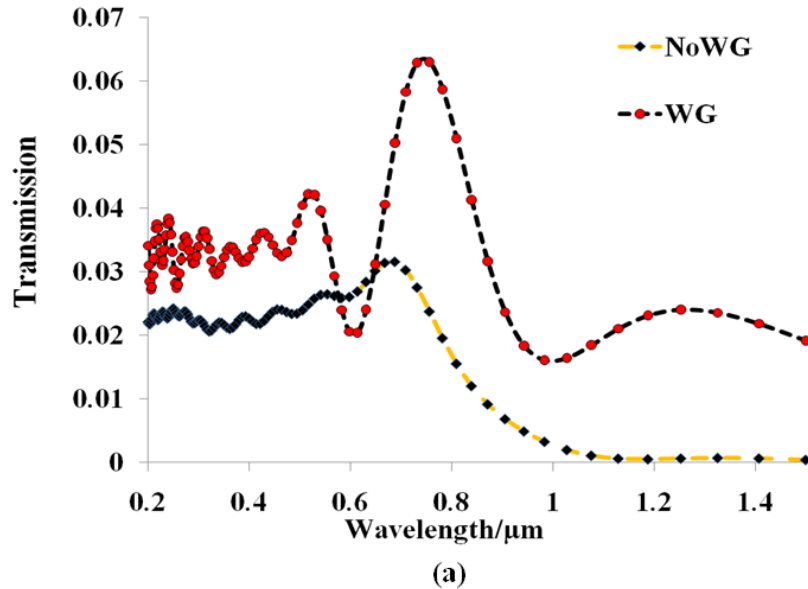


Fig. 4. **a)** Simulated TE-polarization transmission spectra and, **b)** simulated power distribution without (left) and with (right) dielectric waveguide

The TE-polarized light transmission spectra are shown in Figure 4(a), for two optimized MSM-PDs with and without a dielectric waveguide (WG). From these spectra it is obvious that the dielectric waveguide on top of the metal nano-gratings significantly enhanced the TE-polarized light transmission, compared with the conventional MSM-PD device without a dielectric waveguide (NoWG). The resonance wavelength (corresponding to the highest transmission) was 755nm for $\Lambda = 600$ nm and the transmission enhancement was almost 3-times that of a conventional MSM-PD device without a dielectric waveguide.

Moreover, as seen in Figure 4(a), the cut-off wavelength was increased when the slit was filled with the dielectric. The simulated S_x poynting vectors, i.e. energy flowing along the x direction, are shown in Figures 4(b), for the MSM-PD without (left) and with (right) a dielectric waveguide. It is worthwhile noting that for an MSM-PD without a dielectric waveguide, the power transmitted into the active area of the semiconductor is insignificant, compared with the power transmitted for an MSM-PD with a dielectric waveguide.

4. Conclusions

The finite difference time-domain (FDTD) method has been used to optimize the TE-polarized light transmission of a metal-semiconductor-metal photodetector (MSM-PD) employing a dielectric waveguide and metal nano-gratings. Simulation results have confirmed the dependence of the TE-polarized light through the MSM-PD nanoslit of the structure on the metal nano-grating height and dielectric waveguide height. Three-fold enhancement of TE-polarized light transmission has been demonstrated through MDM-PD parameter optimization.

Acknowledgements

We acknowledge the support of Edith Cowan University and the World-Class University Program funded by the Ministry of Education, Science, and Technology through the National Research Foundation of Korea (R31-10026).

References

- [1] Soole, J. and Schumacher, H., InGaAs Metal-Semiconductor-Metal Photodetectors for Long Wavelength Optical Communications. *IEEE J. Q. Elec.*, **27**(3), P. 737–752 (1991).
- [2] Liu, M.Y. and Chou, S.Y., Internal emission metal-semiconductor-metal photodetectors on Si and GaAs for 1.3 μm detection. *Appl. Phys. Lett.*, **66**, P. 2673–2675 (1995).
- [3] Rogers, D. L., Integrated Optical Receivers using MSM Detectors. *J. Lightwave. Technol.*, **9**(Dec.), (1991).
- [4] Averine, S., Chan, Y. C., and Lam, Y. L., Geometry optimization of interdigitated Schottky-barrier metal–semiconductor–metal photodiode structures. *Solid-State Electron.*, **45**(Mar.), P. 441–446 (2001).
- [5] Burm, J., Litvin, K. I., Schaff, W. J., and Eastman, L. F., Optimization of high-speed metal-semiconductor-metal photodetectors. *IEEE Photon. Technol. Lett.*, **6**, P. 722–724 (1994).
- [6] Chou, S. Y., Liu, Y., and Fischer, P. B., Fabrication of sub-50 nm finger spacing and width high-speed metal-semiconductor-metal photodetectors using high-resolution electron beam lithography and molecular beam epitaxy. *J. Vac. Sci. Technol*, **9**(Nov.), P. 2920–2924 (1991).
- [7] Ebbesen, T. W., Lezec, H. J., Ghaemi, H. F., Thio, T., and Wolff, P. A., Extraordinary optical transmission through sub-wavelength hole arrays. *Nature*, **391**(Feb. 12), P. 667–669 (1998).
- [8] Martín-Moreno, L., García-Vidal, F. J., Lezec, H. J., Degiron, A., and Ebbesen, T. W., Theory of Highly Directional Emission from a Single Subwavelength Aperture Surrounded by Surface Corrugations. *Phys. Rev. Lett.*, **90**(25 Apr.), P. 167401 (2003).
- [9] Sondergaard, T., Bozhevolnyi, S. I., Novikov, S. M., Beermann, J., Devaux, E., and Ebbesen, T. W., Extraordinary optical transmission enhanced by nanofocusing. *Nano Lett.*, **10**(Aug. 11), P. 3123–8 (2010).
- [10] Shackelford, J. A., Grote, R., Currie, M., Spanier, J. E., and Nabet, B., Integrated plasmonic lens photodetector. *Appl. Phys. Lett.*, **94**(Feb. 23), P. 083501, P. 1–3 (2009).
- [11] Dunbar, L. A., Guillaume, M., Len-Prez, F. D., Santschi, C., Grenet, E., Eckert, R., Lopez-Tejiera, F., Garcia-Vidal, F. J., Martín-Moreno, L., and Stanley, R. P., Enhanced transmission from a single subwavelength slit aperture surrounded by grooves on a standard detector. *Appl. Phys. Lett.*, **95**(9 Jul.), P. 011113 (2009).
- [12] Karar, A., Das, N., Tan, C.L., Alameh, K., Lee, Y.T., and Karouta, F., High-responsivity plasmonics-based GaAs metal-semiconductor-metal photodetectors. *Appl. Phys. Lett.*, **99**, P. 33112–33112 (2011).

- [13] Ren. F.F., Ang. K.W., Ye. J, Yu., M, Lo. G.Q., and Kwong. D.L., Split Bull's Eye Shaped Aluminum Antenna for Plasmon-Enhanced Nanometer Scale Germanium Photodetector. *Nano Lett.*, **11**, P. 1289-93 (2011).
- [14] Collin. S., Fabrice. P., Teissier. R., and Pelouard. J.-L., Efficient light absorption in metal-semiconductor-metal nanostructures. *Appl. Phys. Lett.*, **85**(Jul.), P. 194-196 (2004).
- [15] Lee. S. C., Krishna. S., and Brueck. S. R. J., Light direction-dependent plasmonic enhancement in quantum dot infrared photodetectors. *Appl. Phys. Lett.*, **97**(Jul. 12), P. 021112 (2010).
- [16] Nikitin. A.Yu., Garcia-Vidal. F.J., and Martin-Moreno. L., Enhanced optical transmission, beaming and focusing through a subwavelength slit under excitation of dielectric waveguide modes. *J. Opt. A: Pure Appl. Opt.*, **11** (2009).
- [17] Guillaume. M., Nikitin. A. Yu., Klein. M.J.K., Dunbar. L.A., Spassov. V., Eckert. R., Martn-Moreno. L., Garca-Vidal. F.J. and Stanley. R.P., Observation of enhanced transmission for s-polarized light through a subwavelength slit. *Opt. Express*, **18**(9), P. 9722-9727 (2010).